# Fourier transform infrared imaging spectroscopic analysis of tissue engineered cartilage: histologic and biochemical correlations

**Minwook Kim**
**Xiaohong Bi**
Hospital for Special Surgery
Musculoskeletal Imaging and Spectroscopy Laboratory
New York, New York 10021

**Walter E. Horton, Jr.**
Northwestern Ohio Universities College of Medicine
Rootstown, Ohio 44272

**Richard G. Spencer**
NIH, National Institute on Aging
Nuclear Magnetic Resonance Unit
Baltimore, Maryland 21224

**Nancy P. Camacho**
Hospital for Special Surgery
Musculoskeletal Imaging and Spectroscopy Laboratory
New York, New York 10021

**Abstract.** The composition of cartilage is predictive of its *in vivo* performance. Therefore, the ability to assess its primary macromolecular components, proteoglycan (PG) and collagen, is of great importance. In the current study, we hypothesized that PG content and distribution in tissue engineered cartilage could be determined using Fourier-transform infrared imaging spectroscopy (FT–IRIS). The cartilage was grown from chondrocytes within a hollow fiber bioreactor (HFBR) system previously used extensively to study cartilage development. FT–IRIS analysis showed a gradient of PG content, with the highest content in the center near the nutritive fibers and the lowest near the interior surface of the HFBR. Further, we found significantly greater PG content in the region near culture medium inflow (45.0%) as compared to the outflow region (24.7%) ($p<0.001$). This difference paralleled the biochemically determined glycosaminoglycan difference of 42.6% versus 27.8%. In addition, FT–IRIS-determined PG content at specific positions within the tissue sections correlated with histologically determined PG content ($R=0.73$, $p=0.007$). In summary, FT–IRIS determination of PG correlates with histological determination of PG and yields quantitatively similar results to biochemical determination of glycosaminoglycan in developing cartilage.  [DOI: 10.1117/1.1922329]

Keywords: Fourier transform infrared imaging spectroscopy; tissue engineering; tissue engineered cartilage; hollow fiber bioreactor; osteoarthritis.

Paper SS04153R received Aug. 2, 2004; revised manuscript received Sep. 22, 2004; accepted for publication Sep. 22, 2004; published online May 27, 2005.

## 1 Introduction

Articular cartilage provides a near-frictionless load-bearing surface for joints.[1,2] It resists compressive forces and distributes loads via interactions between its primary macromolecular components, collagen and proteoglycan (PG).[2,3] Loss of this function occurs as a result of pathological changes in collagen and PG, and can lead to joint degeneration, or osteoarthritis (OA),[4–6] a progressive, potentially immobilizing, disease affecting millions of people.[7] Accordingly, monitoring the molecular composition of cartilage *in vivo* is of great importance.

A significant impediment to the treatment of cartilage degeneration is the lack of methods to diagnose the disease process at an early stage and to assess therapeutic efficacy. Characterizing the tissue matrix and changes in collagen and PG in the greatest possible detail would be a key element of any such evaluation. Magnetic resonance (MR) imaging has emerged as a primary modality for such assessment, with anatomic definition of cartilage on a spatial scale of roughly 100 $\mu$m now being supplemented by use of MR techniques more or less specific for hydration and for collagen and PG content.[8,9] However, to truly characterize the microstructure and biochemistry of cartilage, extraction of tissue for *in vitro* studies is still required. Histological evaluation provides details of microstructural changes, as well as a qualitative indicator of the distribution of macromolecules, by using appropriate stains.[10] Biochemical assays can be used to obtain more quantitative information on collagen and PG content, but with loss of detailed spatial information. Clearly, an *in vivo* technique to obtain quantitative, high resolution compositional and structural information from native and repair cartilage would be invaluable.

In the current study, Fourier transform infrared imaging spectroscopy (FT–IRIS) was used to evaluate the composition of tissue engineered cartilage grown in a hollow fiber bioreactor (HFBR).[11] FT–IRIS is an extension of conventional infrared spectroscopy, whereby an FTIR spectrometer is coupled to an optical microscope equipped with an array detector. The methodology enables the evaluation of the relative amount, molecular nature, distribution, and orientation of the components of tissues.[12] Although the FT–IRIS technology is currently applicable only to *in vitro* analysis, the parallel development of an infrared fiber optic probe to evaluate carti-

Address all correspondence to Nancy P. Camacho. Tel: (212) 606-1435; Fax: (212) 472-5331; E-mail: camachon@hss.edu

1083-3668/2005/$22.00 © 2005 SPIE

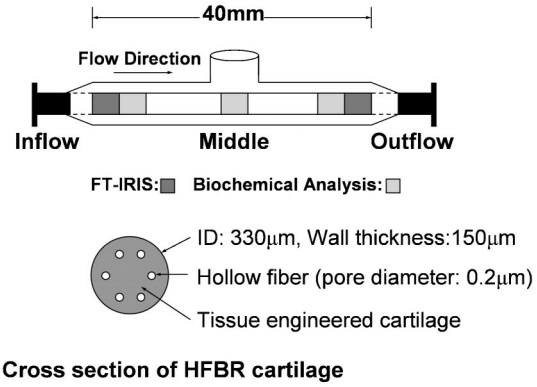


**Fig. 1** Schematic diagram of HFBR (adapted from Chen et al., see Ref. 18). Regions analyzed by FT–IRIS and biochemistry are highlighted.

lage *in vivo*[13] supports the eventual application of the FTIR imaging method to the clinical setting. A detailed understanding of the spatially localized spectra obtained from FT–IRIS is required in order to pursue this comprehensively. Here, we demonstrate the correspondence of FT–IRIS-determined PG content in cartilage to biochemically determined sulfated glycosaminoglycan (S-GAG) content and to histological PG evaluation.

## 2 Materials and Methods

### 2.1 *HFBR Construction and Seeding*

HFBR cartilage was grown from chondrocytes isolated from chick distal sterna as previously described.[14–17] Briefly, the bioreactors were constructed from high purity glass tubing (inner diameter 4 mm, total length 60 mm) which had six porous polypropylene hollow fibers inserted (inner diameter 330 $\mu$m, 0.2 $\mu$m pores, wall thickness 150 $\mu$m). Each bioreactor was inoculated with $3\times10^7$ cells through the rubber septum on the side port. At the end of the 4 week culture period, the HFBR cartilage was removed and sectioned into segments vertical to the fiber axis (Fig. 1). The composition of HFBR cartilage varies according to the proximity to the point of media influx or efflux,[18] and accordingly, analyses were conducted on HFBR cartilage designated as either near the inflow or outflow region. Three to four tissues per group were utilized for FT–IRIS, histology, and biochemical analyses.

### 2.2 *FT–IRIS Analysis*

Tissues were fixed in EtOH and cetylpyridinium chloride (to preserve proteoglycan),[19] embedded in paraffin, sectioned onto barium fluoride windows, and deparaffinized prior to FT–IRIS data acquisition. A BioRad (BioRad, Cambridge, MA) FTS-60A step-scanning Stingray 6000 FTIR spectrometer with a UMA 300A FTIR micrometer and a 64×64 MCT FPA detector (Stingray imaging spectrometer) was used to obtain 4096 FTIR spectra at 8 $cm^{-1}$ spectral resolution under $N_2$ purge. Data were gathered from a 400×400 $\mu m^2$ region at 7 $\mu$m spatial resolution. FT–IRIS data were also collected at 8 $cm^{-1}$ spectral resolution using a Spectrum SpotLight FTIR imaging system (Perkin-Elmer, UK) to obtain IR images of the entire HFBR cartilage cross section. This system consists of an FTIR spectrometer coupled to an optical microscope

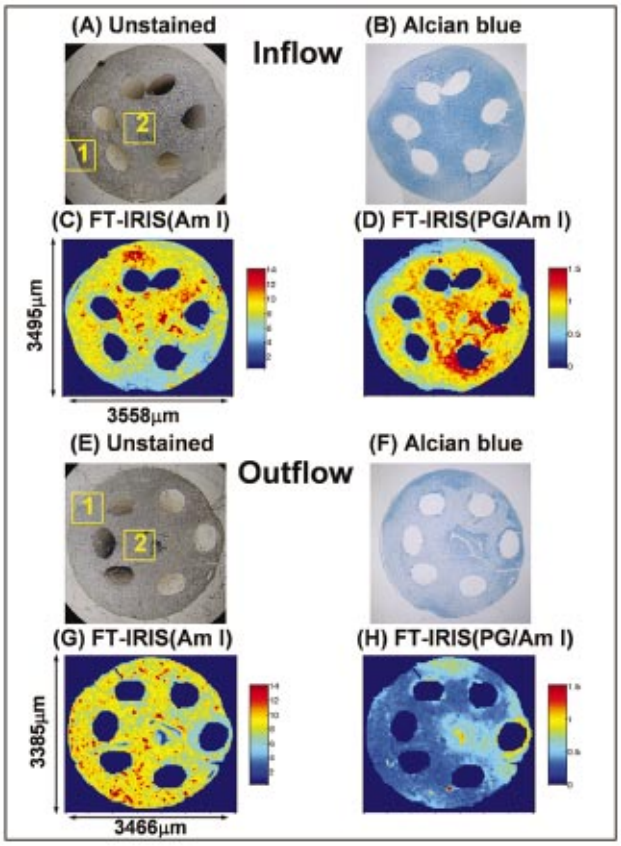


**Fig. 2** Cross sections of inflow and outflow tissue from HFBR cartilage. Unstained sections on barium fluoride windows and histologic Alcian blue-stained sections from inflow (a,b) and outflow (e,f) tissue. FT–IRIS images of inflow (c,d) and outflow (g,h) tissues created based on amide I absorbance and PG/Amide I absorbance, respectively. Regions labeled as "1" and "2" show where data were acquired from the "surface" and "center" of the tissues, respectively.

with a 16×1 linear array of detector elements which has the capability to image a rectangular sample size up to several millimeters in length at a spatial resolution of 6.25 $\mu$m. Typically, images of the whole tissue section were acquired within ~20 min. Data were analyzed with ISys 2.3 software (Spectral Dimensions Inc., Olney, MD). The primary macromolecular components of cartilage, collagen and PG, give rise to specific absorbances in the infrared, as previously described.[20] Integrated absorbance band areas were calculated and utilized as indicators of the quantity of component present. Collagen was monitored in the 1590–1720 $cm^{-1}$ spectral region (amide I absorbance), and proteoglycan [macromolecules consisting of S-GAGs linked to a core protein] in the 985–1140 $cm^{-1}$ spectral region. Absorbances in this region arise from vibrations of the C–O–C and C–OH bonds.[21] Spectra were baselined and images based on the integrated area of the amide I region were created to determine type II collagen quantity and distribution. The ratio of the integrated area of the PG absorbance to the amide I collagen absorbance was evaluated in order to obtain relative quantity and distribution of the PG component (PG/Am I). The PG/Am I data were converted to % PG content based on standard mixtures of pure collagen and the proteoglycan aggrecan.[20] For comparison to histologi-

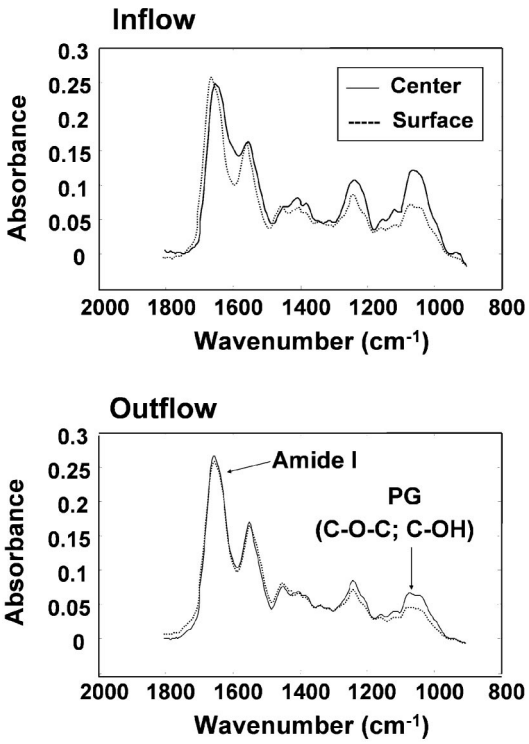


**Fig. 3** FT–IRIS spectra obtained from positions in the center and at the outer surface of inflow and outflow tissue engineered cartilage. There is a greater absorbance in the proteoglycan sugar region (985–1140 $cm^{-1}$) in the center of the tissue versus the surface, although this difference is more pronounced in the inflow tissues as compared to the outflow tissues.

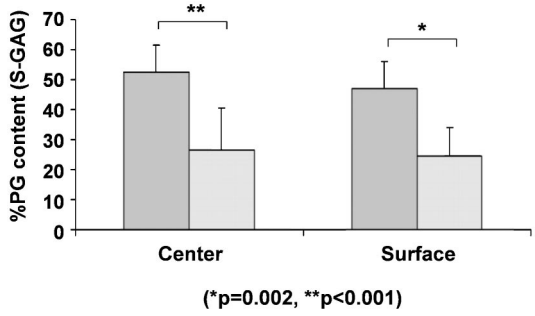


**Fig. 4** Average FT–IRIS-determined % PG content from inflow and outflow tissues at positions in the center and near the surface of the cartilage. Inflow sections showed significantly higher PG content than outflow in both the center and outer surface. (dark shading, inflow; light shading, outflow).

cal data, PG content was quantitated in two regions for each section analyzed, near the cartilage outer surface, and in the center of the tissue [Figs. 2(a) and 2(e)]. For comparison to biochemical data, PG content was quantitated over the whole tissue section.

### 2.3 *Histological Analysis*

Alcian blue-stained sections from the same tissues utilized for FT–IRIS analysis were examined by light microscopy for histological determination of PG content. For each stained section, the integrated optical (IO) density was determined at the same two positions utilized for FT–IRIS analysis, near the outer surface, and in the center of the tissue. Bioquant software (Bioquant Image Analysis Co., Nashville, TN) was used for IO density analysis, where a darker blue color in the extracellular matrix was assumed to arise from a higher PG content.

### 2.4 *Biochemical Analysis*

Tissue segments were harvested from the HFBR cartilage and S-GAG concentration was determined by the dimethylmethylene blue method normalized to dry weight of the tissue.[18,22]

### 2.5 *Statistical Analysis*

A one-way analysis of variance was performed followed by post-hoc tests for comparison of FT–IRIS inflow to outflow data. A paired *t* test was used for comparison of FT–IRIS data at two different positions within the same sample. A Pearson correlation was used to determine significant correlations between FT–IRIS and histology data. All data were analyzed in SigmaStat 2.03 software (SPSS Inc., Chicago, IL) and differences were considered significant at the $p<0.05$ level.

## 3 Results

Distribution of collagen and proteoglycan components in FT–IRIS images of HFBR cartilage inflow and outflow sections are shown in Figs. 2(c), 2(d) and 2(g), 2(h), respectively. Although the collagen (amide I) images are qualitatively similar between the inflow and outflow sections, the PG/Am I images are quite different, with the inflow image reflecting a greater PG content. The Alcian blue-stained sections also reflected this pattern [Figs. 2(b) and 2(f)]. FT–IRIS spectra from regions towards the center of the cartilage and near the surface of the cartilage (adjacent to the HFBR inner surface) illustrate the higher absorbances in the PG sugar region, 985–1140 $cm^{-1}$, for the tissue near the tissue culture medium inflow as compared to tissue near the outflow, and for the tissue near the center of the HFBR as compared to the surface regions, within each of these tissue segments (Fig. 3). Quantitative analysis of the FT–IRIS data revealed a significantly higher PG content in the inflow versus outflow tissues at both positions evaluated, although this difference was more pronounced for the inflow tissues (Fig. 4). Comparison of PG/Am I values to histological determination of PG by integrated optical density calculation showed a significant correlation between these two methods ($R=0.73$, $p=0.007$) (Fig. 5). Biochemical determination of S-GAG content normalized by dry weight showed the highest content in the inflow tissue (42.6%) and the lowest in the outflow tissue (27.8%) [Fig. 6(a)]. Upon conversion of the FT–IRIS-determined PG values from the whole tissue to PG dry weight, the FT–IRIS data showed a similar difference of 45.0% PG in the inflow tissues versus 24.7% in the outflow tissues. However, the correlation between the biochemical and FT–IRIS data did not reach statistical significance due to sample number limitations ($R=0.72$, $p=0.07$) [Fig. 6(b)].

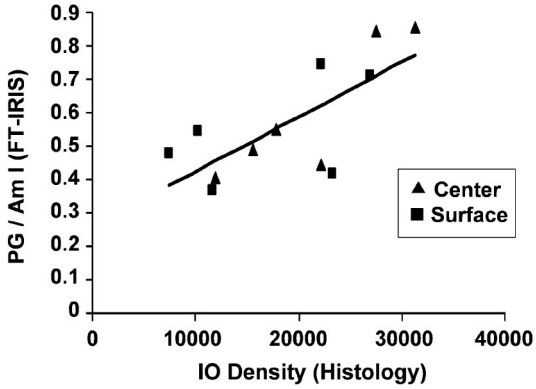


**Fig. 5** Correlation between FT–IRIS-determined % PG content and histologic determination of integrated optical density on Alcian blue-stained sections ($R=0.73$, $p=0.007$). Regions from both the center and the surface of tissue sections were included in the analysis.

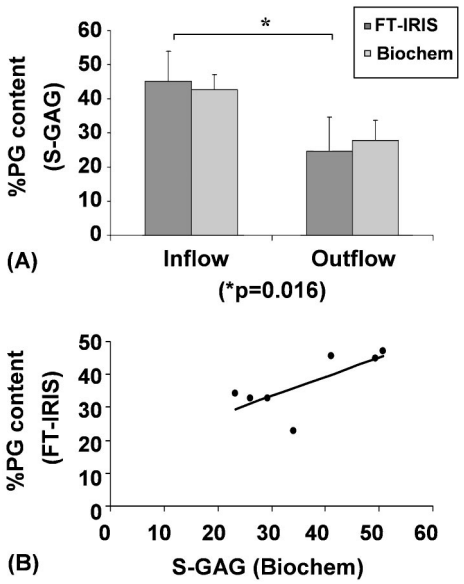


**Fig. 6** (a) FT–IRIS-determined PG content converted to % PG/dry weight compared to biochemical determination of S-GAG content. Mean inflow and outflow values were significantly different by both biochemical and FT–IRIS measurements. In addition, there was no significant difference between biochemical and FT–IRIS-determined values for inflow or outflow tissues. (b) Correlation between FT–IRIS-determined PG content and biochemical S-GAG determination did not reach statistical significance due to sample number limitations ($R=0.72$, $p=0.07$).

## 4 Discussion

Characterization of molecular changes in native, repair, and tissue engineered cartilage is a critical element in the development of therapeutic approaches to OA. Previous studies from our laboratories have monitored type II collagen and PG components in cartilage in a semi-quantitative fashion,[14,20] and the current study now extends that work by evaluation of differences in PG content between biochemically different samples at 6.25 $\mu$m spatial resolution. The current data demonstrate that quantitative FT–IRIS-determined PG content in tissue sections is consistent with bulk biochemical measurements of S-GAG content in tissue engineered cartilage, and correlates with histological determination of PG content in tissue sections. These results support the use of FT–IRIS as an important tool in the development and monitoring of therapeutics for cartilage disorders. Moreover, since FT–IRIS analysis is based on *molecular* alterations in tissue, it may be possible to discern pathologic or therapeutic effects before macroscopic changes are observed.

Cartilage is spatially heterogeneous, and superimposed degradation processes greatly increase heterogeneity. Therefore, it is important to quantitate the molecular composition at high spatial resolution. Historically, evaluation of the spatial distribution of PG content in cartilage has been done by analysis of appropriately stained histologic sections,[23] the most commonly used stains being Safranin O and Alcian blue. Safranin O is a cationic dye that binds stoichiometrically to polyanions, e.g., to the keratin and chondroitin sulfate moieties of proteoglycans.[24] Based on this assumption, this method has been used for semiquantitative analysis of PG content in cartilage.[25–28] However, actual quantification of PG in tissue sections using this method and most other histological methods is challenging due to lack of reproducibility of staining intensity from sample to sample, and to variations of section thickness. Alcian blue staining has also been used frequently to identify PG or hyaline cartilaginous tissue.[29–31] The primary difficulty with this staining method is that the staining intensity is very pH dependent, and also varies with the concentration of ions used in the staining solution.[32] Thus, PG quantification from experiment to experiment can be even more problematic than with Safranin O. To minimize those effects in the current study, the tissue engineered cartilage sections were stained using the same preparation of Alcian blue dye on the same day. In spite of careful preparation, such histological studies are still limited by potential variability in section thickness. Even though all sections were cut at a set thickness of 10 $\mu$m, the actual thickness of the sections can vary by 20% (data not shown) due to inherent limitations in the precision of the microtome. Ultimately, many of the histological studies of PG content, including the one in the current study, evaluate PG content in a relative, and not absolute, manner.

Some of the limitations associated with histological analysis of PG content are avoided by using FT–IRIS to determine PG content. In particular, variations associated with section thickness can be minimized by the inclusion of an appropriate standard,[33] or by normalization of absorbance bands of interest to a standard absorbance band from the tissue embedding medium that is related to section thickness. Alternatively, in the current study, we calculated the ratio of the PG sugar absorbance to the amide I absorbance, thereby factoring out section thickness. Furthermore, these ratios have previously been correlated to specific quantities of aggrecan and collagen mixtures in a series of model compounds.[20]

Another potential strength of the FT–IRIS method is that it monitors PGs based on molecular vibrations, and therefore can reflect changes in molecular structure. Although we currently have only investigated total PG content based on absorbance of the sugar components of the molecule, earlier studies have identified proteoglycans and their components, such as hyaluronic acid, chondroitin-4-sulfate and chondroitin-6-

sulfate, based on differences in spectral features.[34,35] It is very likely that these spectral features will change as the molecular structure of PGs is altered through degradative disease processes,[36] and we envision ultimately being able to utilize the spectral changes to monitor PG degradation.

The morphology and composition of repair and engineered cartilage is likely to be predictive of its ultimate *in vivo* functionality,[37] so that developing the ability to assess these parameters in the clinical setting is of great importance. To date, magnetic resonance imaging (MRI) has been the technique of choice for defining cartilage anatomic features such as volume, thickness and surface characteristics.[38,39] In addition, emerging MRI techniques[9] permit the delineation of more specific biochemical aspects of cartilage matrix, including hydration, PG content,[40] and collagen content. Recently, MRI has also been applied to the evaluation of a model of repair cartilage.[17,18] While it is clear that MRI has the potential for early detection of OA and evaluation of compositional properties of repair tissue, the optimal MRI methods towards these goals have not yet been established. In addition, there are certain limitations inherent to MRI techniques as currently implemented. Chief among these is the relative lack of specificity of several of the MRI outcome measures, in spite of their high sensitivity. In addition, alterations in net matrix composition are likely to occur later than molecular changes in component macromolecules. Finally, the spatial resolution of MRI studies is limited; currently, 100 $\mu$m isotropic resolution would be considered to be beyond realistic clinical capabilities.

In summary, evaluation of native, repair and engineered cartilage at the molecular level is of critical importance, as is development of novel modalities of investigation. The current study demonstrates for the first time that FT–IRIS determination of PG correlates with the gold standard technique of histological determination of PG, and yields quantitatively similar results to biochemical determination. The FT–IRIS technique, and the related fiber optic technology appropriate for clinical use,[13] with its potential for quantitative tissue analysis, sensitivity to early molecular changes, and high degree of spatial resolution, may represent an important approach to clinical cartilage assessment.

## Acknowledgment

This study was supported by NIH EB00744 (N.P.C.).

## References

1. S. L. Carney and H. Muir, ''The structure and function of cartilage proteoglycans (review),'' *Physiol. Rev.* **68**(3), 858–910 (1988).
2. M. Nieminen, J. Toyras, J. Rieppo, J. M. Hakumaki, J. Silvennoinen, H. J. Helminen, and J. Jurvelin, ''Quantitative MR microscopy of enzymatically degraded articular cartilage,'' *Magn. Reson. Med.* **43**(5), 676–681 (2000).
3. J. Rieppo, J. Toyras, M. T. Nieminen, V. Kovanen, M. M. Hyttinen, R. K. Korhonen, J. S. Jurvelin, and H. J. Helminen, ''Structure-function relationships in enzymatically modified articular cartilage,'' *Cells Tissues Organs* **175**(3), 121–132 (2003).
4. H. J. Mankin and K. D. Brandt, ''Pathogenesis of osteoarthritis,'' in *Textbook of Rheumatology*, W. N. Kelley, E. D. Harris, S. Ruddy, and C. B. Sledge, Eds., pp. 1369–1403, WB Saunders Co., Philadelphia (1997).
5. J. Martel-Pelletier, ''Pathophysiology of osteoarthritis (review),'' *Osteoarthritis Cartilage* **12**, S31–S33 (2004).
6. M. Huber, S. Trattnig, and F. Lintner, ''Anatomy, biochemistry, and physiology of articular cartilage (review),'' *Invest. Radiol.* **35**(10), 573–580 (2000).
7. D. W. Jackson, T. M. Simon, and H. M. Aberman, ''Symptomatic articular cartilage degradation: the impact in the new millennium (review),'' *Clin. Orthop.* **391**, S14–S25 (2001).
8. D. Burstein, A. Bashir, and M. L. Gray, ''MRI techniques in early stages of cartilage disease (review),'' *Invest. Radiol.* **35**(10), 622–638 (2000).
9. D. Burstein and M. L. Gray, ''New MRI techniques for imaging cartilage (review),'' *J. Bone Jt. Surg., Am. Vol.* **85-A**(2), 70–77 (2003).
10. Y. H. An and H. E. Gruber, ''Introduction to experimental bone and cartilage histology,'' in *Handbook of Histology Methods for Bone and Cartilage*, Y. H. An and K. L. Martin, Eds., Chap 1, pp. 3–31, Humana Press, Totowa, NJ (2003).
11. E. F. Petersen, K. Potter, J. Butler, K. W. Fishbein, W. E. Horton, R. G. Spencer, and E. W. McFarland, ''Bioreactor and probe system for magnetic resonance microimaging and spectroscopy of chondrocytes and neocartilage,'' *Int. J. Imaging Syst. Technol.* **8**(3), 285–292 (1997).
12. M. J. Friedrich, ''Joint effort: scientists engineer solutions for repairing damaged cartilage,'' *J. Am. Med. Assoc.* **291**(22), 2685–2688 (2004).
13. P. A. West, M. P. Bostrom, P. A. Torzilli, and N. P. Camacho, ''Fourier transform infrared spectral analysis of degenerative cartilage: an infrared fiber optic probe and imaging study,'' *Appl. Spectrosc.* **58**(4), 376–381 (2004).
14. K. Potter, L. H. Kidder, I. W. Levin, E. N. Lewis, and R. G. Spencer, ''Imaging of collagen and proteoglycan in cartilage sections using Fourier transform infrared spectral imaging,'' *Arthritis Rheum.* **44**(4), 846–855 (2001).
15. K. Potter, J. J. Butler, C. Adams, K. W. Fishbein, E. W. McFarland, W. E. Horton, and R. G. Spencer, ''Cartilage formation in a hollow fiber bioreactor studied by proton magnetic resonance microscopy,'' *Matrix Biol.* **17**(7), 513–523 (1998).
16. E. F. Petersen, K. W. Fishebein, E. W. McFarland, and R. G. Spencer, ''$^{31}$P NMP spectroscopy of developing cartilage produced from chick chondrocytes in a hollow-fiber bioreactor,'' *Magn. Reson. Med.* **44**(3), 367–372 (2000).
17. K. Potter, J. J. Butler, W. E. Horton, and R. G. Spencer, ''Response of engineered cartilage tissue to biochemical agents as studied by proton magnetic resonance microscopy,'' *Arthritis Rheum.* **43**(7), 1580–1590 (2000).
18. C. Chen, K. W. Fishbien, P. A. Torzilli, A. Hilger, R. G. Spencer, and W. E. Horton, ''Matrix fixed-charge density as determined by magnetic resonance microscopy of bioreactor-derived hyaline cartilage correlates with biochemical and biomechanical properties,'' *Arthritis Rheum.* **48**(4), 1047–1056 (2003).
19. G. Landemore, M. Quillec, N. Oulhaj, and J. Izard, ''Collagen-associated sulphated proteoglycans. Ultrastructure after formaldehyde-cetylpyridinium chloride fixation,'' *Histochem. J.* **23**(11–12), 534–540 (1991).
20. N. P. Camacho, P. West, P. A. Torzilli, and R. Mendelsohn, ''FT-IR microscopic imaging of collagen and proteoglycan in bovine cartilage,'' *Biopolymers* **62**(1), 1–8 (2001).
21. S. M. Bychkov, V. N. Bogatov, and S. A. Kuz'mina, ''Study of different proteoglycan salts,'' *Biull Eksp Biol. Med.* **92**(9), 302–305 (1981).
22. G. Muller and M. Hanschke, ''Quantitative and qualitative analyses of proteoglycans in cartilage extracts by precipitation with 1,9-dimethylmethylene blue,'' *Connect. Tissue Res.* **33**(4), 243–248 (1996).
23. J. L. Hyllested, K. Veje, and K. Ostergaard, ''Histochemical studies of the extracellular matrix of human articular cartilage (review),'' *Osteoarthritis Cartilage* **10**(5), 333–343 (2002).
24. L. Rosenberg, ''Chemical basis for the histological use of safranin O in the study of articular cartilage,'' *J. Bone Jt. Surg., Am. Vol.* **53**(1), 69–82 (1971).
25. P. Pastoureau, S. Leduc, A. Chomel, and F. De Ceuninck, ''Quantitative assessment of articular cartilage and subchondral bone histology in the meniscectomized guinea pig model of osteoarthritis,'' *Osteoarthritis Cartilage* **11**(6), 412–423 (2003).
26. C. Shimizu, R. D. Coutts, R. M. Healey, T. Kubo, Y. Hirasawa, and D. Amiel, ''Method of histomorphometric assessment of glycosami-

noglycans in articular cartilage,'' *J. Orthop. Res.* **15**(5), 670–674 (1997).
27. M. A. LeRoux, J. Arokoski, T. P. Vail, F. Guilak, M. M. Hyttinen, I. Kiviranta, and L. A. Setton, ''Simultaneous changes in the mechanical properties, quantitative collagen organization, and proteoglycan concentration of articular cartilage following canine meniscectomy,'' *J. Orthop. Res.* **18**(3), 383–392 (2000).
28. S. W. O'Driscoll, R. G. Marx, J. S. Fitzsimmons, and D. E. Beaton, ''Method for automated cartilage histomorphometry,'' *Tissue Eng.* **5**(1), 13–23 (1999).
29. Y. Nishida, A. L. D'Souza, E. J. Thonar, and W. Knudson, ''Stimulation of hyaluronan metabolism by interleukin-1alpha in human articular cartilage,'' *Arthritis Rheum.* **43**(6), 1315–1326 (2000).
30. M. Ramallal, E. Maneiro, E. Lopez, I. Fuentes-Boquete, M. J. Lopez-Armada, J. L. Fernandez-Sueiro, F. Galdo, F. J. De Toro, and F. J. Blanco, ''Xeno-implantation of pig chondrocytes into rabbit to treat localized articular cartilage defects: an animal model,'' *Wound Repair Regen* **12**(3), 337–345 (2004).
31. R. Garimella, X. Bi, N. P. Camacho, J. B. Sipe, and H. C. Anderson, ''Primary culture of rat growth plate chondrocytes: an *in vitro* model of growth plate histotype, matrix vesicle biogenesis and mineralization,'' *Bone (N.Y.)* **34**(6), 961–970 (2004).
32. E. Ippolito, V. A. Pedrini, and A. Pedrini-Mille, ''Histochemical properties of cartilage proteoglycans,'' *J. Histochem. Cytochem.* **31**(1), 53–61 (1983).
33. J. Rieppo, M. M. Hyttinen, J. S. Jurvelin, and H. J. Helminen, ''Reference sample method reduces the error caused by variable cryosection thickness in Fourier transform infrared imaging,'' *Appl. Spectrosc.* **58**(1), 137–140 (2004).
34. S. M. Bychkov and S. A. Kuz'mina, ''Study of tissue proteoglycans by means of infrared spectroscopy,'' *Biull Eksp Biol. Med.* **114**(9), 246–249 (1992).
35. S. M. Bychkov and S. A. Kuz'mina, ''The comparative study of the IR spectra of proteoglycans,'' *Biull Eksp Biol. Med.* **112**(11), 480–482 (1991).
36. M. A. Pratta, M. D. Tortorella, and E. C. Arner, ''Age-related changes in aggrecan glycosylation affect cleavage by aggrecanase,'' *J. Biol. Chem.* **275**(50), 39096–39102 (2000).
37. P. Mainil-Varlet, T. Aigner, M. Brittberg, P. Bullough, A. Hollander, E. Hunziker, R. Kandel, S. Nehere, K. Pritzker, S. Roberts, and E. Stauffer, ''Histological assessment of cartilage repair: a report by the Histology Endpoint Committee of the Internation Cartilage Repair Society (ICRS),'' *J. Bone Jt. Surg., Am. Vol.* **85-A**(2), 45–57 (2003).
38. R. Burgkart, C. Glaser, A. Hyhlik-Durr, K. H. Englmeier, M. Reiser, and F. Eckstein, ''Magnetic resonance imaging-based assessment of cartilage loss in severe osteoarthritis: accuracy, precision, and diagnostic value,'' *Arthritis Rheum.* **44**(9), 2072–2077 (2001).
39. C. G. Peterfy, ''Scratching the surface: articular cartilage disorders in the knee,'' *Magn. Reson Imaging Clin. N. Am.* **8**(2), 409–430 (2000).
40. A. Bashir, M. L. Gray, J. Hartke, and D. Burstein, ''Nondestructive imaging of human cartilage glycosaminoglycan concentration by MRI,'' *Magn. Reson. Med.* **41**(5), 857–865 (1999).